International Journal of Mechanics and Solids.
ISSN 0973-1881 Volume 18, Number 2 (2023), pp. 97-114

https://dx.doi.org/10.37622/IJM&S/18.2.2023.97-114

Three-dimensional MHD Casson Nanofluid Flow Over a Moving Surface in the Presence of Heat Generation and Convective Boundary Conditions

Rekha K.[1], Asha C. S.[2], Achala L. Nargund[3] and S. B. Sathyanarayana[4]

[1, 2 and 3]P. G. Department of Mathematics and Research Centre in Applied Mathematics, M E S College of Arts, Commerce and Science, Malleswaram, Bangalore-560003.
[4]Department of Mathematics, Vijaya College, R V Road, Basavanagudi, Bangalore-560004.

Abstract

The impact of three-dimensional steady incompressible boundary layer flow of Casson nanofluid in the presence of heat generation is scrutinized. The geometry of the present analysis is moving surface. Moreover, we considered the magnetohydrodynamics effect within the fluid and convective condition along the surface. The governing partial differential equations are transformed by using similarity transformation into a set of coupled nonlinear ordinary differential equations. The resulting ordinary differential equations are solved analytically by Homotopy Analysis Method (HAM). The behaviour of emerging parameters is depicted visually and described for velocity, temperature and concentration profiles. It is discovered that increasing the Casson fluid and magnetic field parameters increases the velocity profiles in both the $x-$ and $y-$ directions. Numerical solution is obtained using MATHEMATICA NDSolve technique. Radius of convergence is calculated using Domb-Sykes plot. A comparative study is made with the previous results and observed good agreement.

Keywords: Casson nanofluid, MHD, Heat source, HAM, Domb-Sykes plot.

1 Introduction

Casson fluid model was introduced in 1959 by Casson to characterize non-Newtonian fluid behaviour. Fluids like Jelly, tomato sauce, honey, soup, foams, molten chocolates, cosmetics, nail polish, stuffs, artificial fibers, concentrated fruit liquids are examples for the Casson fluid. Casson fluid model can also be used to treat human blood. Casson

fluid is a shear thinning/thickening liquid which is assumed to have an infinite viscosity at zero rate of shear, a yield stress below which no flow occurs and a zero viscosity at an infinite rate of shear. If the shear stress is less than the applied yield stress on the fluid then Casson fluid act as a solid. If the shear stress is greater than the applied yield stress then it acts as a fluid. The study of Casson fluid has wide applications in food processing, in metallurgy, drilling operations and bio-engineering operations [1, 2].

Wang [14] described the motion of the fluid over a stretching surface in two lateral directions. Mustafa et al. [4] concluded that the Casson parameter increases the velocity field for an unsteady boundary layer flow over a moving plate. The impacts of thermal radiation and heat source of the three-dimensional MHD mixed convection flow of Casson nanofluid over an exponentially stretching sheet is studied by Ibrahim et al. [5]. The boundary layer flow of a Casson fluid model over a stretching sheet in the presence of thermal radiation and velocity slip boundary conditions is investigated by Abdul Hakeem et al. [6]. The laminar flow of a Casson fluid in a curved tube of circular cross-section has been analyzed for large values of Dean number by Batra et al. [7].

The magnetohydrodynamic flow of a Casson fluid over a porous stretching sheet is addressed in the presence of a chemical reaction using HAM is studied by Shehzad et al. [8]. Nagarani et al. [9] studied the dispersion of solute in a Casson fluid flowing in an annulus with interphase mass transfer at the outer boundary. Nawaz et al. [10] analyzed the three-dimensional nano-plasma flow over the two-dimensional stretching surface subject to the applied magnetic field using Galerikan Finite Element Method. The effects of viscous dissipation, thermophoresis, and Brownian motion on the MHD fluid boundary layer in relation to a wedge embedded in porous media is studied by Amar et al. [11]. Mahanthesh et al. [12, 13] analyzed the nonlinear convection in the three-dimensional flow of an Oldroyd-B fluid and water based nanofluid over a non-linearly stretching sheet and numerically solved by using Runge–Kutta–Fehlberg fourth–fifth order method along with shooting technique.

Mahanta et al. [3] investigated the MHD boundary layer three-dimensional flow for Casson fluid model over a stretching sheet and used SRM method for numerical solution. The heat and mass transfer analysis of the steady laminar Casson nanofluid flow over a stretching sheet with velocity slip and convective boundary condition using Optimal HAM are discussed by Abolbashari et al. [15]. Sarojamma et al. [16] analyzed the influence of magnetic field and heat source on the steady boundary layer flow and heat transfer of a Casson nanofluid over a vertical exponentially stretching cylinder along its radial direction and revealed that Skin friction is higher in the Newtonian nanofluid than it is in the Casson nanofluid. Nadeem et al. [17] discussed the MHD boundary layer flow of a Casson fluid over an exponentially permeable shrinking sheet and analytically solved by the Adomian Decomposition Method (ADM).

Rehman et al. [18] discussed the impact of a double stratified medium on Casson fluid flow over a stretching cylindrical surface. The Soret-Dufour properties in mixed convective radiated 3D Casson fluid flow by exponentially heated surface is explained and analytically solved by Homotopic scheme by Zaigham Zia et al. [19]. The double diffusion Cattaneo-Christove flow of Casson nanofluids in a three-dimensional time-dependent magnetohydrodynamic rotation across an extended sheet is investigated by Ali et al. [20]. Sunitha et al. [21] studied the effect of chemical reaction on magnetized

thermally radiant williamson nanofluid over an exponentially stretching sheet using homotopy analysis method.

Anwar et al. [22] investigated the Soret and Dufour effects of Casson nanofluid flow over a nonlinear inclined surface with radiation numerically using Keller−Box method. The heat and mass transfer analysis of magnetized blood flow induced by the peristaltic wave is analyzed by Rashidi et al. [23]. Recently the MHD boundary layer flow of Casson nanofluid in the presence of Brownian motion and thermophoresis properties is solved using HAM by Raj Sekhar et al. [24]. Omowaye et al. [25] studied the Soret and Dufour effects on steady MHD convection flow past a semi-infinite moving vertical plate in a porous using HAM. Gangadhar et al. [26] conducted a detailed study in the flow and heat transfer analysis of three-dimensional steady electrically conducting Casson fluid flow over a porous stretching sheet with source and sink by using spectral relaxation method (SRM).

The three-dimensional nanofluid model proposed by Buongiorno in steady natural convection porous medium presented by Sheremet et al. [27]. The magneto-hydrodynamic fluid flow of the Casson fluid across a nonlinearly stretching sheet in the presence of Newtonian heating and velocity slip is numerically solved by the R-K method with shooting technique by Venkateswara Raju et al.[28]. The three-dimensional flow with nanoparticles over a bi-directional stretching sheet with convective boundary conditions is studied by Khan et al. [29]. The effect of incompressible Casson nanofluid flow past a stretching/shrinking surface with heat radiation and mass transfer parameter is studied by Mahabaleshwar et al. [30]. Recently, Vanitha et al. [31] investigated the unsteady casson nanofluid over a moving surface.

In this paper, we analyzed the magnetohydrodynamic boundary layer flow of three-dimensional Casson nanofluid model with convective boundary conditions and heat generation over a moving surface. We are extending the work of Ahmad et al. [32] for three-dimensional in the presence of heat generation over a moving surface. The distribution of the paper is section 2 includes Mathematical formulation, section 3 contains Method of solution, section 4 involves Results and discussion and section 5 graphs and tables.

2 Mathematical Formulation

The three-dimensional steady incompressible boundary layer flow of Casson nanofluid over a moving surface with heat source and convective boundary conditions are considered. The moving sheet is located at $z = 0$ and the flow is limited to $z \geq 0$. Uniform magnetic field B_0 is applied in $z-$ direction, which is orthogonal to $xy-$ plane. The velocity distribution far from the surface is assumed to be U and V where as velocity of moving surface is λU and λV along $x-$ and $y-$ directions.

The rheological equation of an incompressible flow of a Casson fluid can be written as[33]

$$\tau_{ij} = \begin{cases} 2(\mu_B + \frac{p_z}{\sqrt{2\pi}})e_{ij}, & \pi > \pi_c \\ 2(\mu_B + \frac{p_z}{\sqrt{2\pi_c}})e_{ij}, & \pi < \pi_c \end{cases} \quad (1)$$

where μ_B is dynamic viscosity, p_z be the yield stress, $\pi = e_{ij}.e_{ij}$ is the product of component of deformation tensor with itself, e_{ij} denotes the $(i,j)^{th}$ component of the deformation rate and π_c is the critical value of π.
Under these assumptions the equations of the fluid model are

$$\frac{\partial u}{\partial x}+\frac{\partial v}{\partial y}+\frac{\partial w}{\partial z}=0, \tag{2}$$

$$u\frac{\partial u}{\partial x}+v\frac{\partial u}{\partial y}+w\frac{\partial u}{\partial z}=\nu\left(1+\frac{1}{\beta}\right)\frac{\partial^2 u}{\partial z^2}-\frac{\sigma B_0^2(u-U)}{\rho}, \tag{3}$$

$$u\frac{\partial v}{\partial x}+v\frac{\partial v}{\partial y}+w\frac{\partial v}{\partial z}=\nu\left(1+\frac{1}{\beta}\right)\frac{\partial^2 v}{\partial z^2}-\frac{\sigma B_0^2(v-U)}{\rho}, \tag{4}$$

$$u\frac{\partial T}{\partial x}+v\frac{\partial T}{\partial y}+w\frac{\partial T}{\partial z}=\alpha_m\frac{\partial^2 T}{\partial z^2}+\frac{Q_0}{\rho c_p}(T-T_\infty)+\frac{\rho_p c_p}{\rho c}\left(D_B\frac{\partial C}{\partial z}\frac{\partial T}{\partial z}+\frac{D_T}{T_\infty}\left(\frac{\partial T}{\partial z}\right)^2\right), \tag{5}$$

$$u\frac{\partial C}{\partial x}+v\frac{\partial C}{\partial y}+w\frac{\partial C}{\partial z}=D_B\frac{\partial^2 C}{\partial z^2}+\frac{D_T}{T_\infty}\frac{\partial^2 T}{\partial z^2}. \tag{6}$$

The corresponding boundary conditions are given by

$$u=\lambda U, v=\lambda V, w=0, k\frac{\partial T}{\partial z}=h_f(T-T_w), C=C_w \text{ at } z=0,$$

$$u\to U, v\to V, T\to T_\infty, C\to C_\infty, \text{as } z\to\infty, \tag{7}$$

where u, v and w are velocity components in x, y and z directions, β is Casson fluid parameter, ν is the kinematic viscosity and α_m is the thermal diffusivity of nanofluid, ρ is density of the fluid, σ is the electrical conductivity, τ is heat capacity ratio, D_T is thermophoresis coefficient, B_0 is uniform magnetic field, T is the temperature of the fluid, C is the concentration of the fluid, D_B is Brownian diffusion coefficient, Q_0 is heat source parameter and h_f is convective heat transfer coefficient. Using the similarity transformations

$$u=Uf', v=Ug', w=\left(\frac{U\nu}{2(x+y)}\right)^{\frac{1}{2}}[f'\eta-f-g+g'\eta],$$

$$\theta(\eta)=\frac{T-T_\infty}{T_w-T_\infty}, \phi(\eta)=\frac{C-C_\infty}{C_w-C_\infty}, \eta=z\sqrt{\frac{U}{2\nu(x+y)}}, \tag{8}$$

equations (3)-(6) are reduced to ordinary differential equations as follows.

$$\left(1+\frac{1}{\beta}\right)f'''+(f+g)f''-M(f'-1)=0, \tag{9}$$

$$\left(1+\frac{1}{\beta}\right)g'''+(f+g)g''-M(g'-1)=0,\text{`} \tag{10}$$

$$\theta''+Pr(f+g)\theta'+PrQ\theta+PrNb\theta'\phi'+PrNt(\theta')^2=0, \tag{11}$$

$$\phi''+Le(f+g)\phi'+\frac{Nt}{Nb}\theta''=0. \tag{12}$$

The corresponding boundary conditions are

$$f=0,g=0,f'=\lambda,g'=\lambda\alpha,\theta'=-\gamma[1-\theta],\phi=1\ at\ \eta=0,$$

$$f'\to 1,g'\to\alpha,\theta\to 0,\phi\to 0\ as\ \eta\to\infty. \tag{13}$$

Where α is ratio parameter, $M=\frac{2\sigma B_0^2(x+y)}{\rho U}$; Magnetic field parameter, $Pr=\frac{\nu}{\alpha_m}$; Prandtl number, $\gamma=\frac{h_f}{k}\sqrt{\frac{2\nu(x+y)}{U}}$; Biot number, $Q=\frac{2Q_0(x+y)}{\rho c_p U}$; Heat source parameter, $Le=\frac{\nu}{D_B}$; Lewis number, $Nb=\left(\frac{(\rho c_p)D_B(C_w-C_\infty)}{\nu(\rho c_f)}\right)$; Brownian motion parameter, $Nt=\left(\frac{(\rho c_p)D_T(T_w-T_\infty)}{\nu T_\infty(\rho c_f)}\right)$; Thermophoresis parameter.

3 Method of Solution

Shijun Liao (1992) [34, 35, 36, 37, 38, 39, 40, 41] explained Homotopy Analysis Method (HAM) to solve non-linear differential equations analytically. Using HAM [42, 43], we are proceeding as follows.

The coupled non linear equations for this problem are

$$N[f(\eta)]=\left(1+\frac{1}{\beta}\right)f'''+(f+g)f''-M(f'-1), \tag{14}$$

$$N[g(\eta)]=\left(1+\frac{1}{\beta}\right)g'''+(f+g)g''-M(g'-1), \tag{15}$$

$$N[\theta(\eta)]=\theta''+Pr(f+g)\theta'+PrNb\theta'\phi'+PrQ\theta+PrNt(\theta')^2, \tag{16}$$

$$N[\phi(\eta)]=\phi''+Le(f+g)\phi'+\frac{Nt}{Nb}\theta''. \tag{17}$$

Linear operators considered are as follows,

$$L(f)=\frac{\partial^3 f}{\partial\eta^3}+\frac{\partial^2 f}{\partial\eta^2}, \tag{18}$$

$$L(g)=\frac{\partial^3 g}{\partial\eta^3}+\frac{\partial^2 g}{\partial\eta^2}, \tag{19}$$

$$L(\theta) = \frac{\partial^2 \theta}{\partial \eta^2} + \frac{\partial \theta}{\partial \eta}, \tag{20}$$

$$L(\phi) = \frac{\partial^2 \phi}{\partial \eta^2} + \frac{\partial \phi}{\partial \eta}, \tag{21}$$

which gives initial approximations as,

$$f_0 = (\lambda - 1) + \eta + (1 - \lambda)e^{-\eta}, \tag{22}$$

$$g_0 = \alpha((\lambda - 1) + \eta + (1 - \lambda)e^{-\eta}), \tag{23}$$

$$\theta_0 = \left(\frac{\gamma}{1+\gamma}\right) e^{-\eta}, \tag{24}$$

$$\phi_0 = e^{-\eta}. \tag{25}$$

The nonlinear equations for approximate solutions are,

$$(1 - p)L[f(\eta, p) - f_0(\eta)] = hp[\left(1 + \frac{1}{\beta}\right)\frac{\partial^3 f}{\partial \eta^3} + (f + g)\frac{\partial^2 f}{\partial \eta^2} - M\left(\frac{\partial f}{\partial \eta} - 1\right)], \tag{26}$$

$$(1 - p)L[g(\eta, p) - g_0(\eta)] = hp[\left(1 + \frac{1}{\beta}\right)\frac{\partial^3 g}{\partial \eta^3} + (f + g)\frac{\partial^2 g}{\partial \eta^2} - M\left(\frac{\partial g}{\partial \eta} - 1\right)], \tag{27}$$

$$(1 - p)L[\theta(\eta, p) - \theta_0(\eta)] =$$

$$hp[\frac{\partial^2 \theta}{\partial \eta^2} + Pr(f + g)\frac{\partial \theta}{\partial \eta} + PrNb\frac{\partial \phi}{\partial \eta}\frac{\partial \theta}{\partial \eta} + PrQ\theta + PrNt\left(\frac{\partial \theta}{\partial \eta}\right)^2], \tag{28}$$

$$(1 - p)L[\phi(\eta, p) - \phi_0(\eta)] = hp[\frac{\partial^2 \phi}{\partial \eta^2} + Le(f + g)\frac{\partial \phi}{\partial \eta} + \frac{Nt}{Nb}\frac{\partial^2 \theta}{\partial \eta^2}], \tag{29}$$

with following boundary conditions,

$$f(0, p) = 0, f_\eta(0, p) = \lambda, f_\eta(\infty, p) = 1, \tag{30}$$

$$g(0, p) = 0, g_\eta(0, p) = \lambda\alpha, g_\eta(\infty, p) = \alpha, \tag{31}$$

$$\theta_\eta(0, p) = -\gamma(1 - \theta(0)), \theta(\infty, p) = 0, \tag{32}$$

$$\phi(0, p) = 1, \phi(\infty, p) = 0. \tag{33}$$

Varying the values of p from 0 to 1 we get the solution from first approximation to required solution. Using Maclaurin's series expansion and applying Leibnitz theorem we get the series solution. The convergence of the series solution is derived by

calculating the convergence parameter h.

$$L[f_k - \chi_k f_{k-1}] = hR_k(\eta), \tag{34}$$

$$L[g_k - \chi_k g_{k-1}] = hS_k(\eta), \tag{35}$$

$$L[\theta_k - \chi_k \theta_{k-1}] = hW_k(\eta), \tag{36}$$

$$L[\phi_k - \chi_k \phi_{k-1}] = hX_k(\eta), \tag{37}$$

$$\text{where } \chi_k = \begin{cases} 0, & \text{when } k \leq 1 \\ 1, & \text{when } k > 1 \text{ and} \end{cases} \tag{38}$$

$$R_k(\eta) = \left(1 + \frac{1}{\beta}\right) f'''_{k-1}(\eta) + \sum_{m=0}^{k-1} (f_{k-1-m}(\eta) + g_{k-1-m}(\eta)) f''_m(\eta) - M f'_{k-1}(\eta), \tag{39}$$

$$S_k(\eta) = \left(1 + \frac{1}{\beta}\right) g'''_{k-1}(\eta) + \sum_{m=0}^{k-1} (f_{k-1-m}(\eta) + g_{k-1-m}(\eta)) g''_m(\eta) - M g'_{k-1}(\eta), \tag{40}$$

$$W_k(\eta) = \theta''_{k-1}(\eta) + Pr \sum_{m=0}^{k-1} (f_{k-1-m}(\eta) + g_{k-1-m}(\eta)) \theta'_m(\eta) + PrQ\theta_{k-1}(\eta) +$$

$$PrNb \sum_{m=0}^{k-1} \theta'_{k-1-m}(\eta) \phi'_m(\eta) + PrNt \sum_{m=0}^{k-1} \theta'_{k-1-m}(\eta) \theta'_m(\eta), \tag{41}$$

$$X_k(\eta) = \phi''_{k-1}(\eta) + Le \sum_{m=0}^{k-1} (f_{k-1-m}(\eta) + g_{k-1-m}(\eta)) \phi'_m(\eta) + \frac{Nt}{Nb} \theta''_{k-1}(\eta), \tag{42}$$

with boundary conditions,

$$f_k(0) = 0, f'_k(0) = 0, f'_k(\infty) = 0, \tag{43}$$

$$g_k(0) = 0, g'_k(0) = 0, g'_k(\infty) = 0, \tag{44}$$

$$\theta'_k(0) - \gamma \theta_k(0) = 0, \theta_k(\infty) = 0, \tag{45}$$

$$\phi_k(0) = 0, \phi_k(\infty) = 0. \tag{46}$$

Soving eqution (34)-(37) by using MATHEMATICA we get the required solution as

$$f = f_0 + f_1 + f_2 + f_3 + \ldots, \tag{47}$$

$$g = g_0 + g_1 + g_2 + g_3 + \ldots, \tag{48}$$

$$\theta = \theta_0 + \theta_1 + \theta_2 + \theta_3 + \ldots, \tag{49}$$

$$\phi = \phi_0 + \phi_1 + \phi_2 + \phi_3 + \ldots. \tag{50}$$

Where

$$f_1 = -\frac{-4h + h\beta + 4hM\beta + 5h\alpha\beta + 4h\lambda + 2h\beta\lambda - 4hM\beta\lambda - 2h\alpha\beta\lambda - 3h\beta\lambda^2 - 3h\alpha\beta\lambda^2}{4\beta} +$$

$$\frac{1}{4\beta}e^{-2\eta}(-2e^{2\eta}hM\beta\eta^2 - h(1+\alpha)\beta(-1+\lambda)^2 - 2e^{\eta}(-2h - 3h\beta + 2hM\beta - h\alpha\beta + 2h\lambda +$$

$$6h\beta\lambda - 2hM\beta\lambda + 4h\alpha\beta\lambda - 3h\beta\lambda^2 - 3h\alpha\beta\lambda^2 + h(-1+\lambda)(-2(2+\eta) +$$

$$\beta(-2 + \eta^2 + 2M(2+\eta) + 4\lambda + 2\eta\lambda +$$

$$\alpha(2 + \eta^2 + 4\lambda + 2\eta(1+\lambda))))))\ldots \quad (51)$$

$$g_1 = -\frac{1}{4\beta}(-4h\alpha + h\alpha\beta + 4hM\alpha\beta + 5h\alpha^2\beta + 4h\alpha\lambda + 2h\alpha\beta\lambda - 4hM\alpha\beta\lambda$$
$$- 2h\alpha^2\beta\lambda - 3h\alpha\beta\lambda^2 - 3h\alpha^2\beta\lambda^2) + \frac{1}{4\beta}e^{-2\eta}(-2e^{2\eta}hM\alpha\beta\eta^2$$
$$- h\alpha(1+\alpha)\beta(-1+\lambda)^2 - 2e^{\eta}(-2h\alpha - 3h\alpha\beta +$$

$$2hM\alpha\beta - h\alpha^2\beta + 2h\alpha\lambda + 6h\alpha\beta\lambda - 2hM\alpha\beta\lambda + 4h\alpha^2\beta\lambda - 3h\alpha\beta\lambda^2 -$$

$$3h\alpha^2\beta\lambda^2 + h\alpha(-1+\lambda)(-2(2+\eta) + \beta(-2 + \eta^2 + 2M(2+\eta) + 4\lambda + 2\eta\lambda +$$

$$\alpha(2 + \eta^2 + 4\lambda + 2\eta(1+\lambda))))))\ldots \quad (52)$$

$$\theta_1 = \frac{1}{2(1+\gamma)^2}e^{-2\eta}(h\mathrm{Pr}\gamma(-1-\gamma + \mathrm{Nt}\gamma + \mathrm{Nb}(1+\gamma) + \alpha(1+\gamma)(-1+\lambda) + \lambda + \gamma\lambda)$$
$$+ e^{\eta}(1+\gamma)(-2(1$$
$$+ \gamma)(\frac{h\mathrm{Pr}\gamma(-1-\gamma + \mathrm{Nt}\gamma + \mathrm{Nb}(1+\gamma) + \alpha(1+\gamma)(-1+\lambda) + \lambda + \gamma\lambda)}{2(1+\gamma)^2}$$
$$+ \frac{h\gamma(-2 + \mathrm{Pr}(-2Q + 2(1+\alpha)\lambda))}{2(1+\gamma)}) + h\gamma(-2(1+\eta) + \mathrm{Pr}(-2Q(1+\eta) +$$

$$(1+\alpha)(\eta^2 + 2\lambda + 2\eta\lambda)))))\ldots \quad (53)$$

$$\phi_1 = \frac{1}{2\mathrm{Nb}(1+\gamma)}e^{-2\eta}(h\mathrm{LeNb}(1+\alpha)(1+\gamma)(-1+\lambda) + e^{\eta}(-2\mathrm{Nb}(1+\gamma)(\frac{1}{2}h\mathrm{Le}(1+$$
$$\alpha)(-1+\lambda) + \frac{h(-2\mathrm{Nt}\gamma + 2\mathrm{Nb}(1+\gamma)(-1+\mathrm{Le}(1+\alpha)\lambda))}{2\mathrm{Nb}(1+\gamma)}) + h(-2\mathrm{Nt}\gamma(1+\eta) + \mathrm{Nb}(1+$$
$$\gamma)(\mathrm{Le}(1+\alpha)\eta^2 + 2(-1 + \mathrm{Le}(1+\alpha)\lambda) + 2\eta(-1 + \mathrm{Le}(1+\alpha)\lambda)))))\ldots \quad (54)$$

4 Results and Discussion

The semi-analytical solutions of non-dimensional equations (9)-(12) are obtained by Homotopy Analysis Method. Figure 1 describes the combine $h-$ curve of $f''(0)$,

$g''(0)$, $\theta'(0)$ and $\phi'(0)$. Figures 2 and 3 shows that increasing values of Casson parameter β increases the velocity profiles in $x-$ and $y-$ directions. From figures 4 and 5 we observed that increase in wall moving parameter λ increases the velocity profile $f'(\eta)$ and $g'(\eta)$. From figures 6 and 7, we can see that increase in ratio parameter α increases the velocity fields in both the directions. Here when $\alpha = 0$ the flow reduces to two-dimensional case.The impact of Magnetic parameter M on velocity distributions $f'(\eta)$ and $g'(\eta)$ are shown in the figures 8 and 9.The raise in Magnetic parameter raises the velocity profile due to Casson fluid which opposes the Lorentz force.

Figure 10 represents increase in wall moving parameter λ decreases temperature distribution $\theta(\eta)$. From figure 11 it is observed that larger values of ratio parameter α drops the temperature field $\theta(\eta)$. From figure 12 we observed that increase in Magnetic parameter M decreases the temperature profile $\theta(\eta)$. Figure 13 presents that larger values of Prandtl number Pr leads to lower the temperature field $\theta(\eta)$. The fact that the Prandtl number has an inverse relationship with thermal diffusivity, implying that increased values of Pr correspond to reduction in the thermal diffusivity which leads to the decreasing attitude of fluid temperature. The increase in the heat source parameter Q raises the temperature distribution $\theta(\eta)$ due to increased heat generation in the thermal boundary layer seen in figure 14. The increase in values of Biot number γ, Brownian motion parameter Nb and Thermophoresis parameter Nt increases the temperature profile $\theta(\eta)$ as shown in figures 15, 16 and 17.

From figures 18, 19, 20, 21 and 23, it is observed that the increase in values of wall moving parameter λ, ratio parameter α, Magnetic parameter M, Lewis number Le and Brownian motion parameter Nb decreases the concentration profile $\phi(\eta)$, where as from figure 22 we can observe that increase in Thermophoresis parameter Nt increases the concentration profile $\phi(\eta)$. Radius of convergence for series solution of $f(\eta)$, $g(\eta)$, $\theta(\eta)$ and $\phi(\eta)$ are obtained from Domb-Sykes plot shown in figures 24, 25, 26 and 27. The analytical solution using HAM is compared with numerical solution using MATHEMATICA NDSolve technique are shown in graphs 28 and 29. Also we compared our solutions with existing solution of Ahmad et al. [31] and we observe that in the limiting cases our values matches with their values as shown in the table 1.

5 Graphs and Tables

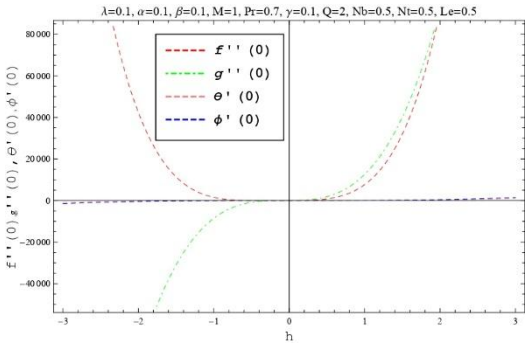

Figure 1: h-curves for the functions f, g, θ and ϕ

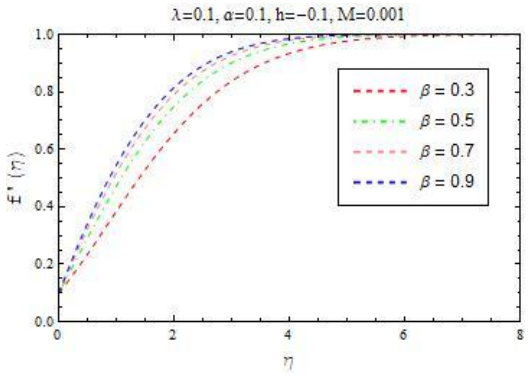

Figure 2: Influence of Casson parameter β on $f'(\eta)$

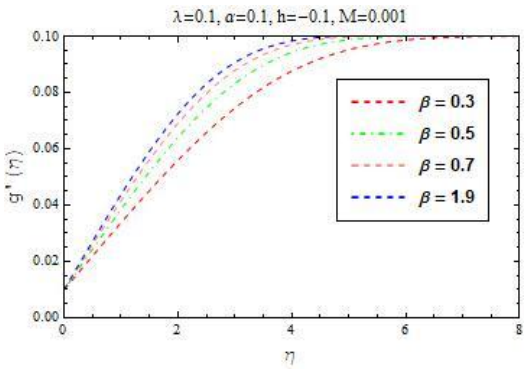

Figure 3: Influence of Casson parameter β on $g'(\eta)$

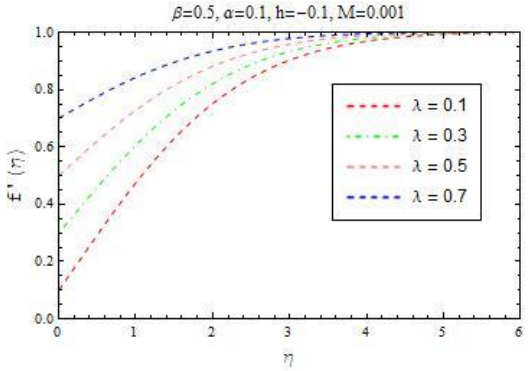

Figure 4: Influence of velocity parameter λ on $f'(\eta)$

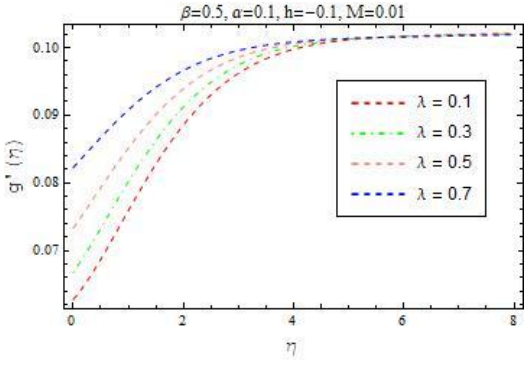

Figure 5: Influence of velocity parameter λ on $g'(\eta)$

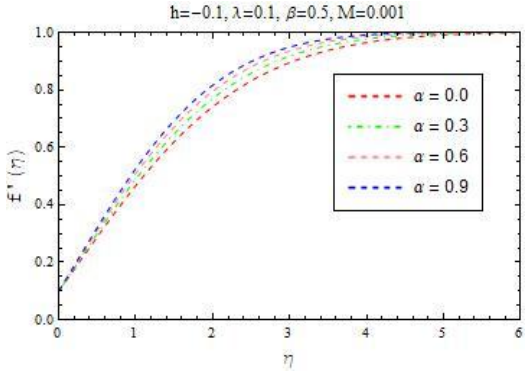

Figure 6: Influence of ratio parameter α on $f'(\eta)$

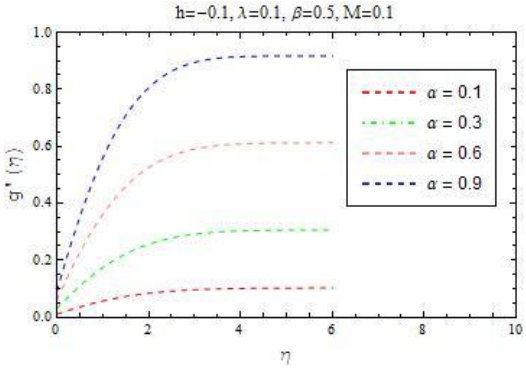

Figure 7: Influence of ratio parameter α on $g'(\eta)$

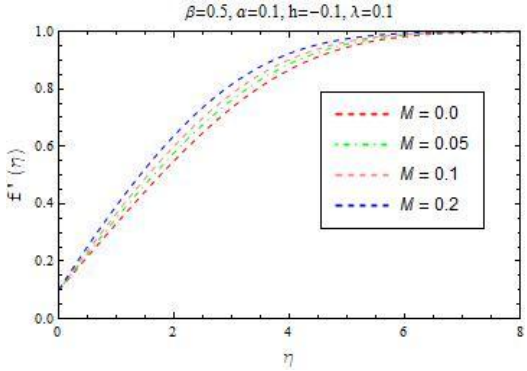

Figure 8: Influence of Magnetic parameter M on $f'(\eta)$

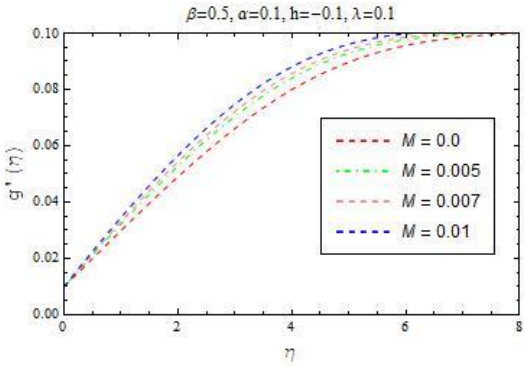

Figure 9: Influence of Magnetic parameter M on $g'(\eta)$

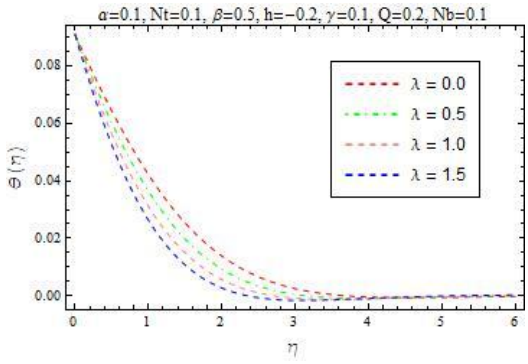

Figure 10: Influence of velocity parameter λ on $\theta(\eta)$

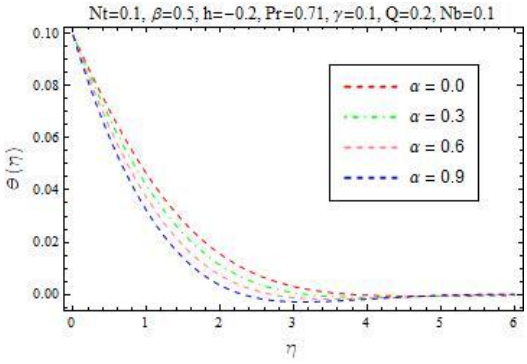

Figure 11: Influence of ratio parameter α on $\theta(\eta)$

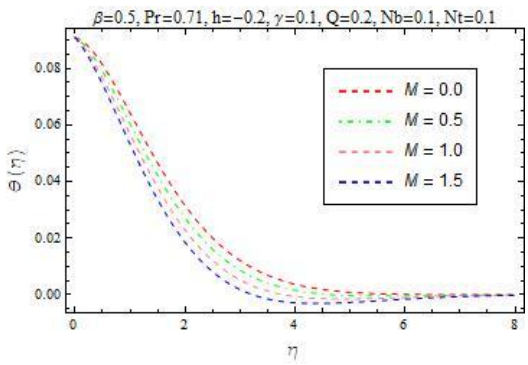

Figure 12: Influence of Magnetic parameter M on $\theta(\eta)$

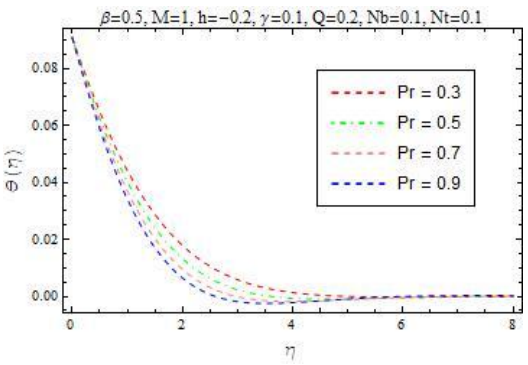

Figure 13: Influence of Prandtl number Pr on $\theta(\eta)$

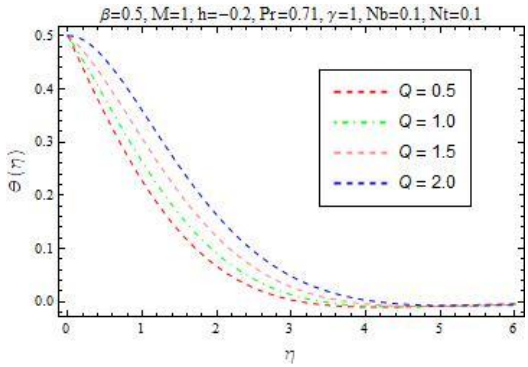

Figure 14: Influence of Heat source parameter Q on $\theta(\eta)$

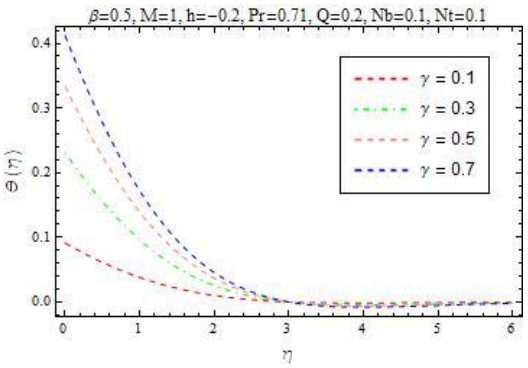

Figure 15: Influence of Biot number γ on $\theta(\eta)$

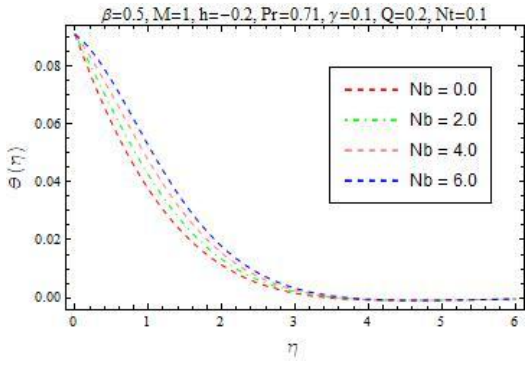

Figure 16: Influence of Brownian motion parameter Nb on $\theta(\eta)$

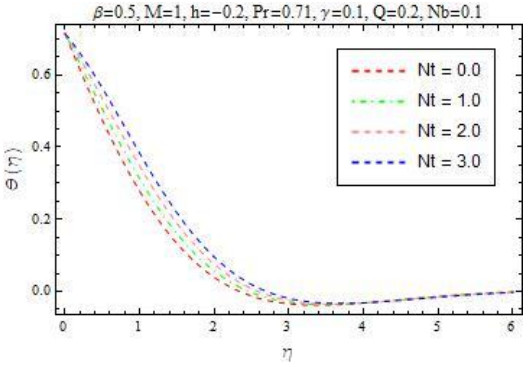

Figure 17: Influence of Thermophoresis parameter Nt on $\theta(\eta)$

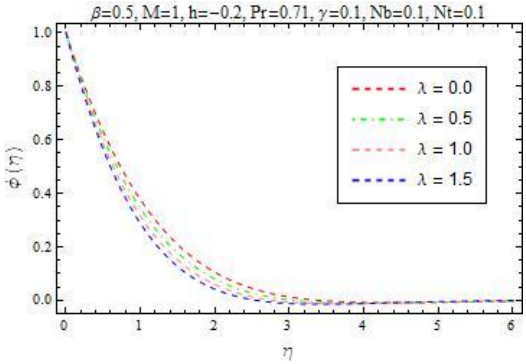

Figure 18: Influence of velocity parameter λ on $\phi(\eta)$

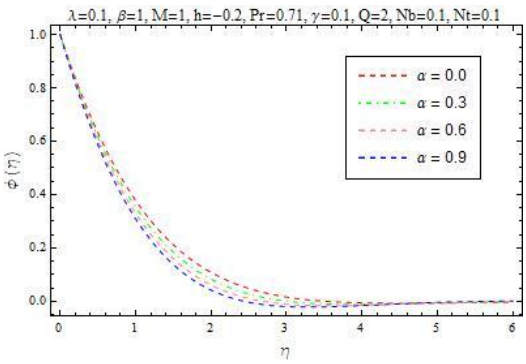

Figure 19: Influence of ratio parameter α on $\phi(\eta)$

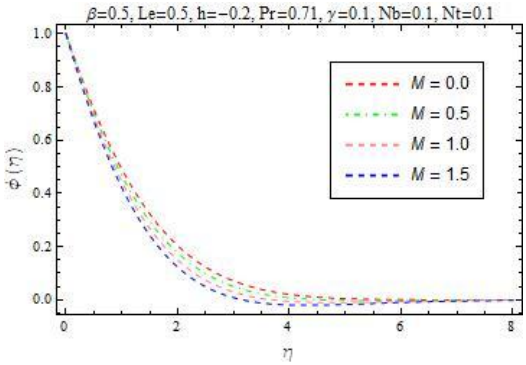

Figure 20: Influence of Magnetic parameter M on $\phi(\eta)$

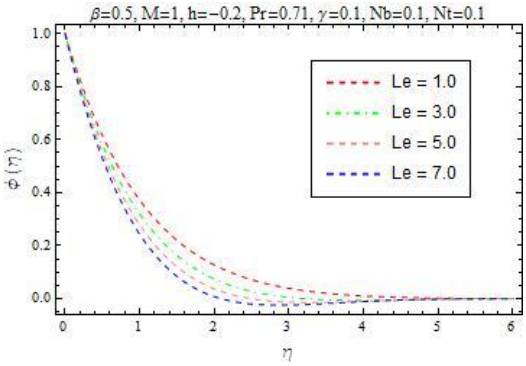

Figure 21: Influence of Lewis number Le on $\phi(\eta)$

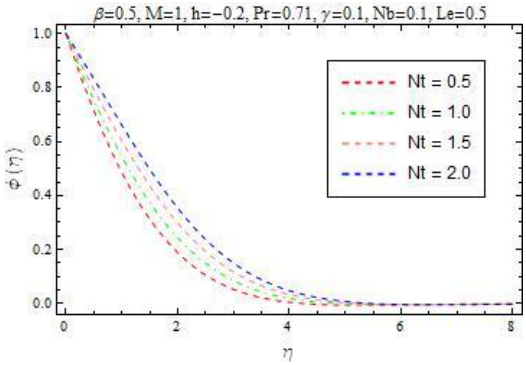

Figure 22: Influence of Thermophoresis parameter Nt on $\phi(\eta)$

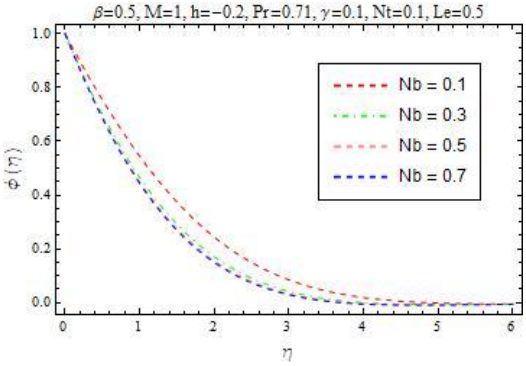

Figure 23: Influence of Brownian motion parameter Nb on $\phi(\eta)$

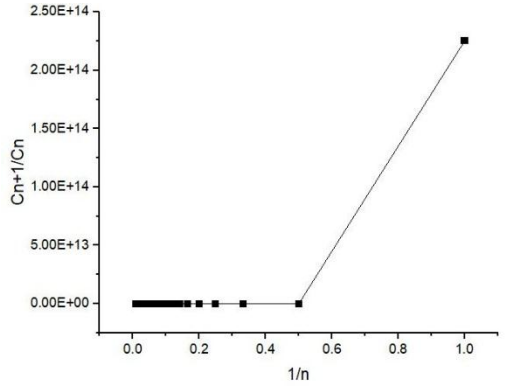

Figure 24: Domb-sykes plot for f with $R = 7.47261$

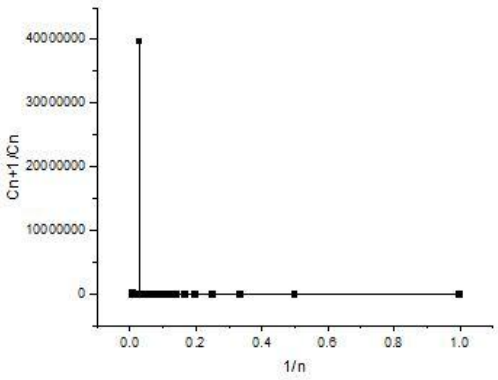

Figure 25: Domb-sykes plot for g with $R = 0.03123$

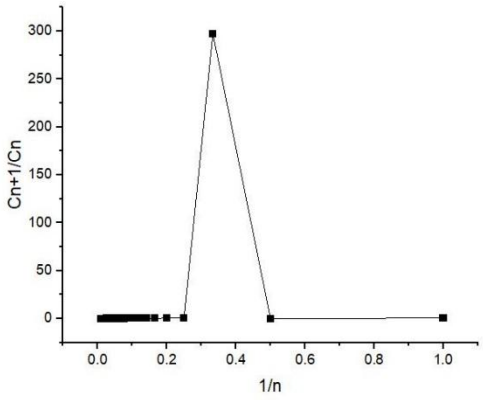

Figure 26: Domb-sykes plot for θ with $R = 26.53223$

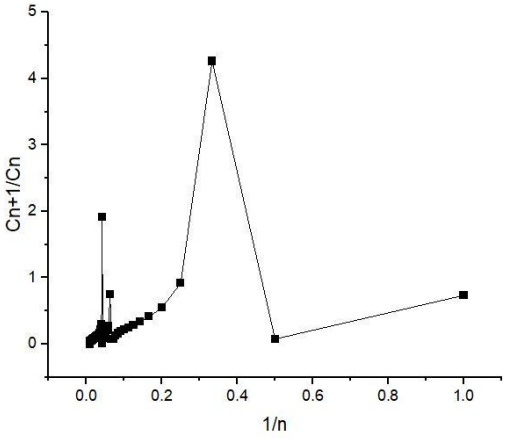

Figure 27: Domb-sykes plot for ϕ with $R = 21.24495$

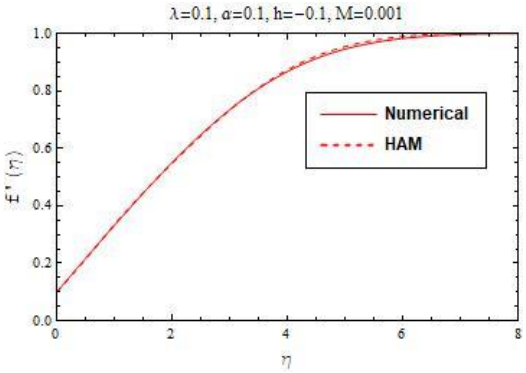

Figure 28: Comparison of HAM and Numerical solution for velocity field

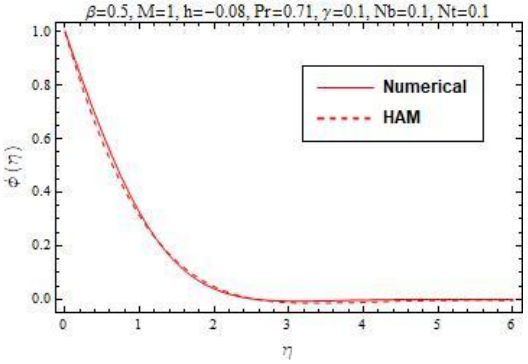

Figure 29: Comparison of HAM and Numerical solution for concentration field

Table 1: Comparision of $f''(0)$ when $\lambda = \alpha = M = 0$ and $h = -0.3$

Parameter	$f''(0)$	
β	Ahmad et al. [32]	Present work
5	0.4696	0.469558

References

[1] Chaturani, P. and Palanisamy, V., Cassson fluid model for pulsatile flow of blood under periodic body acceleration, *Biorheology*, vol. 27, 1990, 619-630.

[2] Dash, R. K., Mehta, K. N., and Jayaraman, G., Casson fluid flow in a pipe filled with a homogeneous porous medium, *International Journal of Engineering Science*, vol. 34(10), 1996, 1145–1156.

[3] Wang, C. Y., The three-dimensional flow due to a stretching flat surface, *Physics of Fluids*, Vol.27, No. 8, 1984, 1915–1917.

[4] Mustafa, M., Hayat, T., Pop, I. and Aziz A., Unsteady boundary layer flow of a Casson fluid due to an impulsively started moving flat plate, *Heat Transfer—Asian Research*., 40(6), 2011, 563–576.

[5] Ibrahim, W. and Anbessa, T., Three-Dimensional MHD Mixed Convection Flow of Casson Nanofluid with Hall and Ion Slip Effects, *Mathematical Problems in Engineering*, Vol. 2020, 2020, 1-15.

[6] Abdul Hakeem, A.K., Renuka, P., Vishnu Ganesh, N., Kalaivanan, R. and Ganga, B., Influence of inclined Lorentz forces on boundary layer flow of Casson fluid over an impermeable stretching sheet with heat transfer, *Journal of Magnetism and Magnetic Materials*, 401, 2016, 354–361.

[7] Batra, R.L. and Bigyani Jena, Flow of a Casson fluid in a slightly curved tube, *International Journal of Engineering and Sciences*, Vol. 29, No. 10, 1991, 1245–1258.

[8] Shehzad, S. A., Hayat, T., Qasim, M. and Asghar, S., Effects of mass transfer on MHD flow of casson fluid with chemical reaction and suction, *Brazilian Journal of Chemical Engineering*, Vol. 30, No. 1, 2013, 187–195.

[9] Nagarani, P., Sarojamma, G. and Jayaraman, G., Effect of boundary absorption on dispersion in Casson fluid flow in an annulus: application to catheterized artery, *Acta Mech*, 202(1-4), 2009, 47–63.

[10] Nawaz, M. and Zubair, T. Finite element study of three-dimensional radiative nano-plasma flow subject to Hall and ion slip currents, *Results in Physics*, Vol. 7, 2017, 4111–4122.

[11] Amar, N and Kishan, N. The influence of radiation on MHD boundary layer flow past a nano fluid wedge embedded in porous media, *Partial Differential Equations in Applied Mathematics*, Vol. 4, 2021, 100082.

[12] Mahanthesh, B., Gireesha, B. J. and Rama Subba Reddy Gorla., Nonlinear radiative heat transfer in MHD three-dimensional flow of water based nanofluid over a non-linearly stretching sheet with convective boundary condition, *Journal of the Nigerian Mathematical Society*, 2016, 1-21.

[13] Mahanthesh, B., Gireesha, B. J., Shehzad, S. A., Abbasi, F. M. and Gorla, R. S. R., Nonlinear three-dimensional stretched flow of an Oldroyd-B fluid with convective condition, thermal radiation, and mixed convection, Applied Mathematics and Mechanics, Vol. 38, No. 7, 2017, 969-980.

[14] Mahanta, G. and Shaw, S., 3D Casson fluid flow past a porous linearly stretching sheet with convective boundary condition, *Alexandria Engineering Journal*, 54, 2015, 653-659.

[15] Abolbashari, M. H., Nazari, N. F. F. and Rashidi, M. M.. Analytical modeling of entropy generation for Casson nano-fluid flow induced by a stretching surface, *Advanced Powder Technology*, 2015, 1-11.

[16] Sarojamma, G. and Vendabai, K., Boundary Layer Flow of a Casson Nanofluid past a Vertical Exponentially Stretching Cylinder in the Presence of a Transverse Magnetic Field with Internal Heat Generation/Absorption, *International Journal of Mathematical and Computational Sciences,* Vol. 9, No. 1, 2015, 138-143.

[17] Nadeem, S., Ul Haq, R. and Lee, C., *MHD flow of a Casson fluid over an exponentially shrinking sheet*, *Scientia Iranica*, Vol. 19, No. 6, 2012, 1550–1553.

[18] Rehman K. U., Malik, A. A., Malik, M. Y. and Saba, N. U., Numerical study of double stratification in Casson fluid flow in the presence of mixed convection and chemical reaction, *Results in Physics*, Vol. 7, 2017, 2997–3006.

[19] Zaigham Zia, Q.M., Ullah, I., Waqas, M., Alsaedi, A. and Hayat, T., Cross diffusion and exponential space dependent heat source impacts in radiated three-dimensional (3D) flow of Casson fluid by heated surface, *Results in Physics*, Vol. 8, 2018, 1275–1282.

[20] Ali, B., Rizwan Ali, N., Amir, H., Dildar, H. and Sajjad, H., Finite Element Study of MHD Impacts on the Rotating Flow of Casson Nanofluid with the Double Diffusion Cattaneo—Christov Heat Flux Model, Vol. 8, No. 9, 2020, 1555.

[21] Sunitha, C., Vijaya Kumar, P., Lorenzini, G. and Ibrahim, S. M., A Study of Thermally Radiant Williamson Nanofluid Over an Exponentially Elongating Sheet with Chemical Reaction Via Homotopy Analysis Method, *CFD Letters*, Vol. 14, No. 5, 2022, 68-86.

[22] Anwar, A. I., Rafique, K., Misiran, M. and Khan, I., Numerical Solution of Casson Nanofluid Flow over a Nonlinear Inclined Surface with Soret and Dufour Effects by Keller-Box Method, *Frontiers in Physics*, Vol. 7, 2019.

[23] Rashidi, M. M., YANG, Z., BHATTI M. M. and ABBAS M. A., Heat and Mass Transfer Analysis On MHD Blood Flow Of Casson Fluid Model Due To Peristaltic Wave, *Thermal Science*, Vol. 22, No. 6A, 2018, 2439-2448.

[24] Raja Sekhar, P., Sreedhar, S., Ibrahim, S. M. and Vijaya Kumar, P. Radiative Heat Source Fluid Flow of MHD Casson Nanofluid over A Non-Linear Inclined Surface with Soret and Dufour Effects, *CFD Letters*, Vol. 15, No. 7, 2023, 42-60.

[25] Omowaye, A.J., Fagbade, A.I. and Ajayi, A.O., Dufour and soret effects on steady MHD convective flow of a fluid in a porous medium with temperature dependent viscosity: Homotopy analysis approach, *Journal of the Nigerian Mathematical Society*, 2015, 1-18.

[26] Gangadhar, K., Subba Rao, M. V., Venkata Ramana, K., Suresh Kumar, Ch., and Chamkha, A. J., Thermal Slip Flow of a Three-Dimensional Casson Fluid Embedded in a Porous Medium with Internal Heat Generation, *Journal of Nanofluids*, Vol. 10, 2021, 58–66.

[27] Sheremet, M.A., Pop, I., Rahman, M.M., Three-dimensional natural convection in a porous enclosure filled with a nanofluid using Buongiorno's mathematical model, *International Journal of Heat and Mass Transfer*, Vol. 82, 2015, 396–405

[28] Venkateswara Raju, K., Durga Prasad, P., Raju, M. C. and Sivaraj, R., MHD Casson Fluid Flow Past a Stretching Sheet with Convective Boundary and Heat Source, *Advances in Fluid Dynamics, Lecture Notes in Mechanical Engineering*, 2021, 559-572.

[29] Khan, Junaid Ahmad, Mustafa, M., Hayat, T., Farooq, M. Asif, Alsaedi, A. and Liao, S.J., On model for three-dimensional flow of nanofluid: An application to solar energy, *Journal of Molecular Liquids*, Vol. 194, 2014, 41–47.

[30] Mahabaleshwar, U. V., Maranna, T. and Sofos, F., Analytical investigation of an incompressible viscous laminar Casson fluid flow past a stretching/shrinking sheet, *Scientific Reports*, Vol. 12, No. 18404, 2022.

[31] Vanitha, G. P., Shobha K. C., Patil Mallikarjun, B., Mahabaleshwar, U. S. and Gabriella Bognár., Casson nanoliquid film flow over an unsteady moving surface with time_varying stretching velocity, *Scientific Reports*, Vol. 13, No. 4074, 2023, 1-13.

[32] Ahmad, K., Hanouf, Z. and Ishak, A, MHD Casson nanofluid flow past a wedge with Newtonian heating, *Eur. Phys. J. Plus*, Vol. 132, No. 87, 2017, 1-11.

[33] Hayat, T., Shehzad, S. A., Alsaedi, A. and Alhothuali, M. S., Mixed Convection Stagnation Point Flow of Casson Fluid with Convective Boundary Conditions, *Chinese Physics Letters*, Vol. 29, No. 11, 2012, 114704.

[34] Liao, S.J., *Advances in the homotopy analysis method*, World Scientific Publishing Co. Pte. Ltd., 2013.

[35] Liao, S.J., *Beyond Perturbation: Introduction to the Homotopy Analysis Method*, Chapman and Hall/CRC Press, Boca Raton, 2003.

[36] Liao, S.J., On the homotopy analysis method for nonlinear problems, *Journal of Applied Mathematics and Computation*, vol. 147, 2004, 499-513.

[37] Liao, S.J., Comparision between the homotopy analysis method and homotopy perturbation method, *Applied Mathematics and Computations*, vol. 169, 2005, 1186-1194.

[38] Achala, L.N. and Sathyanarayana, S.B., Homotopy Analysis Method For Nonlinear Boundary Value Problems, *JP of Applied Mathematics*, Vol. 5, Issues 1 & 2, 2012, 27-46.

[39] Sathyanarayana, S.B. and Achala, L.N., Approximate Analytical Solution of Magnetohydrodynamics Compressible Boundary Layer flow with Pressure Gradient and suction/injection, *Journal of Advances in Physics*, Vol. 6, No. 3, 2014.

[40] Achala, L.N., Madusudhan, R. and Sathyanarayana, S.B., Homotopy Analysis Method To Solve Boussinesq Equations, *Journal of Advances in Physics*, Vol. 10, No. 3, 2015, 2825-2833.

[41] Sushma, V.J., Raju B. T., Achala, L.N. and Sathyanarayana, S.B., MHD boundary layer flow of nanofluid over a moving surface in presence of thermal radiation by homotopy analysis method, *Global Journal of Engineering Science and Researches*, 2019, 435-443.

[42] Rekha, K., Asha, C.S. and Achala, L.N., Williamson Nanofluid Flow over a Moving Surface on Boundary Layer by Homotopy Analysis Method, *International Journal of Mechanical Engineering*, vol.7, No.2, 2022, 1723–1736.

[43] Rekha, K., Asha, C. S. and Achala, L. N., Magnetohydrodynamic Boundary Layer Flow of Williamson Nanofluid over a Moving Surface in the presence of Gyrotactic Microorganism, *International Journal of Mechanics and Thermodynamics*, Vol. 13, No. 1, 2022, 15-31.